Feshbach projection-operator formalism applied to resonance scattering on Bargmann-type potentials

Varvara V. Shamshutdinova,[1,2] Konstantin N. Pichugin,[2,3] Ingrid Rotter,[2] and Boris F. Samsonov[1]
[1]*Tomsk State University, 36 Lenin Avenue, 634050 Tomsk, Russia*
[2]*Max Planck Institute for the Physics of Complex Systems, D-01187 Dresden, Germany*
[3]*Kirensky Institute of Physics, 660036 Krasnoyarsk, Russia*
(Received 27 September 2008; published 16 December 2008)

The projection-operator formalism of Feshbach is applied to resonance scattering in a single-channel case. The method is based on the division of the full function space into two segments, internal (localized) and external (infinitely extended). The spectroscopic information on the resonances is obtained from the non-Hermitian effective Hamilton operator H_{eff} appearing in the internal part due to the coupling to the external part. As is well known, additional so-called cutoff poles of the S matrix appear, generally, due to the truncation of the potential. We study the question of spurious S matrix poles in the framework of the Feshbach formalism. The numerical analysis is performed for exactly solvable potentials with a finite number of resonance states. These potentials represent a generalization of Bargmann-type potentials to accept resonance states. Our calculations demonstrate that the poles of the S matrix obtained by using the Feshbach projection-operator formalism coincide with both the complex energies of the physical resonances and the cutoff poles of the S matrix.

DOI: 10.1103/PhysRevA.78.062712 PACS number(s): 03.65.Nk, 03.65.Fd, 11.30.Pb

I. INTRODUCTION

The Feshbach projection operator (FPO) formalism [1,2] is a powerful method for the description of resonant scattering and reactions involving light nuclei [3,4]. In recent years the FPO technique has been applied to numerous other systems like quantum dots and microwave cavities [5–11] and atoms in a laser field [12–14]. In its original formulation, the formalism is based on the introduction of projection operators Q and P, $QP=PQ=0$, $P+Q=1$, which project, respectively, onto the discrete states of a closed system and the continuous spectrum of a reservoir when their interaction is neglected. Resonance states then naturally appear as bound states of the former closed system embedded into a continuum of open channels, due to the coupling really existing between the closed system and the reservoir. In other words: the starting point of the FPO formalism is the assumption that the scattering event is confined to a certain compact part of the available space [15]. This region constitutes the so-called interaction region and can be described by the Q subspace. Outside this region (in the P subspace) the interaction is absent so that the motion of scattering fragments depends (apart from the total energy E) only on their internal states. Each combination of internal states of all fragments is called a channel of reaction since it specifies a set of configurations (depending on E) in which the system can be found long before and long after the scattering takes places.

The FPO formalism exploits the concept of an effective Hamiltonian H_{eff} to describe the open system resulting from the interaction between the idealized closed system and the reservoir. The operator H_{eff} is, naturally, non-Hermitian and depends explicitly on energy. Its complex eigenvalues z_λ are energy dependent. The solutions of the fixed-point equations for the eigenvalues provide approximately both energy positions and inverse lifetimes (widths) of resonance states [3]. Using the FPO formalism, an expression for the S matrix can be derived [4]. It contains the complex eigenvalues z_λ with their full energy dependence. The energy dependence is important especially in the neighborhood of decay thresholds and in the regime of overlapping resonances [16,17].

As it is well known, analytic properties of the S matrix are very sensitive to both the detailed form of the potential and the behavior of the potential at infinity. Even at a point where the potential equals to zero with a computer precision, the truncation strongly affects the picture, especially the number of the S-matrix poles. In the simple case of the scattering by a potential of a compact support, i.e., a potential vanishing outside a given cutoff radius, the S matrix has an infinite number of discrete poles in the lower part of the complex k plane [18–20] whereas an exponential asymptotic form of the potential can lead to a finite number of poles (see, e.g., [21]). This means that for a truncated potential one obtains not only physical (resonance) S-matrix poles but also so-called cutoff poles [22]. These poles are not an artefact; they are correct poles of the truncated potential but do not cause the characteristic phase shift by π. Therefore there is a need to distinguish between the two kinds of poles [22]. One way to do so is to use the fact that the positions of the resonance poles are not affected by changing the model parameters such as, for instance, the cutoff radius. From a mathematical viewpoint both types of poles are correct but they have different origins. This is the reason why the problem of separation of cutoff poles from the resonance poles is widely discussed in the literature devoted to the S matrix.

To the best of the authors' knowledge the emergence of spurious complex eigenvalues has received little attention in the context of the FPO formalism [23,24]. We think that the reason for that may reside in the fact that some authors (e.g., [25]) find the concept of the non-Hermitian effective Hamiltonian unsuitable in the case of potential scattering. In our opinion, however, the problem is not investigated in necessary details and the current paper is just devoted to fill in this gap.

To avoid unnecessary complications we apply, in the present paper, the FPO formalism to resonance scattering in

its simplest form by considering only single-channel (elastic) *s*-wave scattering. In doing so we exclude the appearance of the Feshbach (core excited) resonance states that are present in the general case (see, e.g., [26]). Thus only potential (shape) resonances may appear in our approach. We assume the potential to have a finite number of resonance states and the continuous spectrum to fill the positive semiaxis resulting as solutions of the usual radial Schrödinger equation. We construct exactly solvable potentials by applying the method of supersymmetric quantum mechanics (SUSY QM) [27] to the inverse scattering problem (see, e.g., Refs. [21,28]). By exact solvability we mean the situation when solutions of the Schrödinger equation are available in an explicit form and, in particular, are expressed in terms of elementary functions.

It is the authors' opinion that the potentials, the scattering data of which we set ourselves, represent a good testing ground for numerous schemes of resonance calculations. Such calculations show the substantial relevance of the concept of the non-Hermitian effective Hamiltonian to resonance scattering on a finite range potential. We show that in this case the FPO formalism gives very accurate results both for the scattering phase shift and the positions and widths of physical resonances as well as for the cutoff poles of the scattering matrix. We discuss the fitness range of the fixed-point approximation and omit from our discussions the question of why the estimation of position and width of the resonance states by this method might be meaningful. In calculations for concrete reactions by using the FPO method, this approximation is never used since the S matrix contains the energy dependent functions $z_\lambda(E)$. It does *not* contain the energy-independent values that characterize the positions and widths of the resonance states and are obtained from, e.g., the solutions of the fixed-point equations [16,17]. In the present paper, we determine the poles of the S matrix exactly within the FPO formalism and compare them with the results of the exactly solvable potentials.

The paper is organized as follows. In Sec. II we recall the methods of SUSY quantum mechanics in the context of scattering theory and construct Bargmann-type potentials supporting resonance states. Using the standard procedures of quantum scattering theory in Sec. III, we calculate the S-matrix poles for truncated Bargmann-type potentials. In Sec. IV, we write down the basic equations of FPO formalism used in the paper. Our numerical scheme for the computation is mainly based on the consideration of quantum scattering on billiards with one attached lead [5]. This model is formulated in the tight-binding approximation (Anderson model). In Sec. V we present numerical results obtained by using the two considered methods. In the last section some conclusions are drawn.

II. BARGMANN-TYPE POTENTIALS SUPPORTING RESONANCE STATES

As it is known, the SUSY approach, when restricted to the derivation of new exactly solvable quantum problems, is basically equivalent to the Darboux transformation method (see, e.g., Ref. [29]). Therefore we use SUSY and Darboux transformations as synonyms. The whole class of potentials known as Bargmann-type potentials (see [30]) may be obtained from the zero potential with the help of either usual SUSY transformations or their confluent forms (see [31–33]). Typically, such a potential has an exponentially decreasing tail and supports a finite number of bound states and no resonances. Its S matrix (as well as the Jost function) is a rational function of the momentum k (see, e.g., [20]). Any such potential may be obtained by a proper chain of SUSY transformations with *real factorization constants* (see the next section for details). Nevertheless, as it is shown in [34], the use of *complex factorization constants* in higher order transformations [35] (see also [36]) may lead to a real potential and corresponds to an irreducible supersymmetry. The use of such SUSY transformations permits us to enlarge the class of standard Bargmann potentials by including potentials supporting resonance states.

A. Darboux transformation method

In this section we shortly recall the definition and main properties of the Darboux transformations method necessary for subsequent analysis. The interested reader can find a more detailed exposition elsewhere [29,31–41].

In its pragmatic formulation the method essentially consists in getting solution φ of the (transformed) differential (Schrödinger) equation

$$h_1\varphi = E\varphi, \quad h_1 = -\frac{d^2}{dr^2} + V_1(r), \tag{1}$$

by applying differential transformation operator L of the form

$$L = -d/dr + w(r), \tag{2}$$

to a known solution ψ of another (initial) equation

$$h_0\psi = E\psi, \quad h_0 = -\frac{d^2}{dr^2} + V_0(r), \tag{3}$$

$\varphi = L\psi$, corresponding to the same value of the parameter E. Here the real-valued function $w(r)$ called the superpotential is defined as the logarithmic derivative of a known solution to Eq. (3) denoted by u

$$w = u'(r)/u(r), \quad h_0 u = \alpha u \tag{4}$$

with $\alpha \leqslant E_0$, where E_0 is the ground state energy of the Hamiltonian h_0 if it has a discrete spectrum or the lower bound of the continuous spectrum otherwise. Function u is called the transformation or factorization function and α is known as the factorization constant or factorization energy. The potential V_1 is defined in terms of the superpotential w as

$$V_1(r) = V_0(r) - 2w'(r). \tag{5}$$

The knowledge of all two-dimensional solution space of the initial equation with a given value of $E \in \mathbb{C}$ provides the knowledge of all solutions of the transformed equation corresponding to the same value of E. In particular, if all solutions for E belonging to the spectrum of h_0 are known (so-called physical eigenfunctions of h_0) the method provides us with all physical eigenfunctions of h_1.

Since the above procedure does not depend on a particular choice of the potential V_0, the transformed Hamiltonian h_1 can play the role of the initial Hamiltonian for the next transformation step. In this way one gets a chain of exactly solvable Hamiltonians $h_0, h_1, \ldots, h_n$ with the potentials $V_0, V_1, \ldots, V_n$. To avoid any confusion we mention that everywhere, except for especially mentioned cases, we shall use subscripts to distinguish between quantities related to different Hamiltonians, $h_0, h_1, \ldots$ and shall omit them when discussing general properties regarding all Hamiltonians.

First-order Darboux transformation operator $L_{j,j+1}$, as defined by Eq. (2), relates solutions of two Hamiltonians h_j and h_{j+1}. If one is not interested in the intermediate Hamiltonians $h_1, \ldots, h_{n-1}$ and all factorization energies are chosen to be different from each other, the whole chain may be replaced by a single transformation given by an nth-order transformation operator, denoted by $L^{(n)}$, defined as a superposition of n first-order transformation operators. A compact representation of this operator is given by [42]

$$\psi_n(r,k) = L^{(n)}\psi_0(r,k) = W(u_1, \ldots, u_n, \psi_0(r,k))W^{-1}(u_1, \ldots, u_n), \tag{6}$$

where $\psi_0(r,k)$ is a solution to Eq. (3) corresponding to the energy $E=k^2$ and $\psi_n(r,k)$ satisfies

$$h_n\psi_n(r,k) = E\psi_n(r,k), \quad E = k^2. \tag{7}$$

The transformation functions u_j, although labeled by a subscript, are eigenfunctions of the initial Hamiltonian

$$h_0 u_j(r) = \alpha_j^2 u_j(r). \tag{8}$$

These should be chosen in a way that the Wronskian $W(u_1, \ldots, u_n)$ is nodeless and either real or purely imaginary for $r \in (0, \infty)$. These conditions guarantee the absence of singularities in the potential

$$V_n = V_0 - 2\frac{d^2}{dr^2} \ln W(u_1, \ldots, u_n) \tag{9}$$

defining the Hamiltonian h_n of Eq. (7) and its real character for $r \in (0, \infty)$. In particular, factorization constants should be either real or come in complex conjugate pairs with corresponding factorization solutions being either real or in pairs complex conjugate to each other. Formula (6) is valid for any $E=k^2$ except for $k=\alpha_j$ $(j=1, \ldots, n)$. For these values of k the corresponding solutions are

$$\psi_n(r,\alpha_j) = W^{(j)}(u_1, \ldots, u_n)W^{-1}(u_1, \ldots, u_n), \tag{10}$$

where $W^{(j)}(u_1, \ldots, u_n)$ is the $(n-1)$st order Wronskian constructed from $u_1, \ldots, u_n$ except for u_j, $j=1, \ldots, n$.

B. Jost function for a special chain of transformations

Let us choose the following set [41] of eigenfunctions of the Hamiltonian h_0 (8) as transformation functions for the Darboux transformation of order $2n$:

$$u_1(r), v_1(r), u_2(r), v_2(r), \ldots, u_n(r), v_n(r), \tag{11}$$

$$h_0 u_j(r) = \alpha_j^2 u_j(r), \quad h_0 v_j(r) = \beta_j^2 v_j(r). \tag{12}$$

Here α's and β's should be different from each other and chosen in a way that the corresponding factorization energies, if they are real, are smaller than the ground state energy of h_0 when it has a discrete spectrum, or less than the lower bound of the continuous spectrum otherwise. No such restrictions are imposed on α's and β's for complex factorization energies.

We distinguish between the functions u and v from their behavior at the origin. The functions v are regular, $v_j(0)=0$, and hence are uniquely defined up to a constant factor, that is not essential for our purpose. The functions u_j are irregular at the origin, $u_j(0) \neq 0$, and form the so-called singular family.

In [41] it was shown that the chain of transformations with transformation functions (11) transforms the initial Jost function $F_0(k)$ of Hamiltonian h_0 to the Jost function,

$$F_n(k) = F_0(k)\prod_{j=1}^{n} \frac{k-\alpha_j}{k+ib_j}, \quad \beta_j \equiv ib_j, \tag{13}$$

corresponding to the Hamiltonian h_n. Since the Jost function should be analytic in the upper half of the complex k plane (see Refs. [21–28]) all b's must be real and positive. This avoids the appearance of the so-called redundant poles, which occur as poles of the Jost function or zeros of the S matrix. Every purely imaginary $\alpha_j = ia_j$ with $a_j > 0$ corresponds to a discrete level $E_j = -a_j^2$ of h_n. No restriction, except the ones discussed above, is imposed on α's. Complex α's coming in pairs with real parts of opposite signs may correspond to a visible resonance. Thus we say that every pair of complex numbers $\alpha_j = \pm \mathrm{Re}[\alpha_j] + i\mathrm{Im}[\alpha_j]$ corresponds to a resonance and to mirror resonance states with complex energy,

$$E_j^{res} = (\pm \mathrm{Re}[\alpha_j] + i\ \mathrm{Im}[\alpha_j])^2 \tag{14}$$

$$= (\mathrm{Re}[\alpha_j]^2 - \mathrm{Im}[\alpha_j]^2) \pm 2i\mathrm{Re}[\alpha_j]\mathrm{Im}[\alpha_j]. \tag{15}$$

In this case, in accordance with the analytic properties of the Jost function (13), the technique developed in [41] remains stable for $\mathrm{Re}[\alpha_j] < 0$, and $\mathrm{Im}[\alpha_j] < 0$. States with $|\mathrm{Re}[\alpha_j]| > |\mathrm{Im}[\alpha_j]|$ correspond to visible resonances provided $\mathrm{Re}[\alpha_j]^2 - \mathrm{Im}[\alpha_j]^2$ is small enough [43].

In the one-channel case the S matrix is a single-valued function of wave number k,

$$S = \frac{F(-k)}{F(k)} = e^{2i\delta(k)}. \tag{16}$$

In our approach $F_n(k)$ differs from $F_0(k)$ by a rational function of momentum k. Therefore the expression for phase shift $\delta_n(k)$ becomes rather complicated when the number of transformation functions is sufficiently large. An alternative expression, which is more convenient for practical calculations, is [41]

$$\delta_n = \delta_0 - \sum_{j=1}^{n} \arctan\left(\frac{k}{-i\alpha_j}\right) - \sum_{j=1}^{n} \arctan\left(\frac{k}{b_j}\right). \quad (17)$$

In Sec. V we apply the above described technique to obtain potentials with either one or two resonance states. Moreover, since our starting potential equals zero, when the usual technique of Darboux transformations [41] reproduces Bargmann potentials [30], the potentials from Sec. V are their generalizations to describe resonance scattering. Below we will denote them by V_{Brg}. It is worthwhile to note that the solutions of the Schrödinger equation for these potentials are expressed in terms of elementary (trigonometric) functions.

III. *S*-MATRIX POLES FOR TRUNCATED BARGMANN POTENTIALS

In order to compare the results obtained by means of the FPO technique and those obtained by the Darboux method we investigate the scattering on truncated Bargmann potentials V_{cut}, i.e., on potentials equal to Bargmann potentials V_{Brg} for $r<R_{cut}$, and equal to zero for $r\geqslant R_{cut}$. In this case, as it is well known, the analytic continuation of $S(k)$ to the complex k plane is a meromorphic function with infinitely many poles. In order to calculate their positions and widths we use the methods of usual quantum scattering theory (see, e.g., [20,44]).

For $r\geqslant R_{cut}$, where $V_{cut}(r)=0$, the solution of Schrödinger equation (1) is a linear combination of plane waves, which we write as

$$\Psi_{r\geqslant R_{cut}} = \cos(\delta_{cut})\sin(kr) + \sin(\delta_{cut})\cos(kr). \quad (18)$$

We denote the phase shift for the truncated potential as δ_{cut}. The phase shift δ_{cut} is obtained by solving Eq. (1) for function $\Psi_{r<R_{cut}}(r)$ in the region $r<R_{cut}$ and matching it to have form (18) at $r=R_{cut}$. Function $\Psi_{r<R_{cut}}(r)$ subject to the Dirichlet boundary condition $\Psi_{r<R_{cut}}(0)=0$, is uniquely defined (up to an inessential constant factor). Although at $r=R_{cut}$ both $\Psi_{r<R_{cut}}$ and $d\Psi_{r<R_{cut}}/dr$ must be continuous, it is sufficient for our purposes to impose continuity on the logarithmic derivative (see, e.g., [44]),

$$\gamma \equiv \left[\frac{1}{\Psi_{r<R_{cut}}}\frac{d\Psi_{r<R_{cut}}}{dr}\right]_{r=R_{cut}} = \left[\frac{1}{\Psi_{r\geqslant R_{cut}}}\frac{d\Psi_{r\geqslant R_{cut}}}{dr}\right]_{r=R_{cut}}, \quad (19)$$

which is independent of a multiplicative constant. From here we find the phase shift of the cutoff potential

$$\tan[\delta_{cut}(k)] = \frac{k\cos(kR_{cut}) - \gamma\sin(kR_{cut})}{k\sin(kR_{cut}) + \gamma\cos(kR_{cut})} \quad (20)$$

which, upon using Eq. (16), gives its S matrix

$$S_{cut}(k) = e^{2i\delta_{cut}(k)} = e^{-2ikR_{cut}}\frac{k-i\gamma}{k+i\gamma}. \quad (21)$$

The poles of $S_{cut}(k)$ are the roots of the transcendental equation

$$\gamma = ik \quad (22)$$

which we solve numerically in Sec. V.

IV. FESHBACH PROJECTION OPERATOR APPROACH TO POTENTIAL SCATTERING

A. Basic relations of FPO formalism

As was mentioned in the Introduction, in the FPO formalism [1,2] the full function space is divided into two subspaces: the Q subspace contains all wave functions that are localized inside the idealized closed system and vanish outside of it while the wave functions of the P subspace are extended up to infinity and vanish inside the system; see [16,17]. This division is carried out by using the projection operators Q and P ($QP=0=PQ$, $P+Q=1$). The wave functions of the two subspaces can be obtained by standard methods: the Q subspace is described by eigenfunctions of Hermitian Hamiltonian H_b that characterizes the localized closed system with a discrete spectrum, while the P subspace is described by the states of Hermitian Hamiltonian H_c, which has a continuous spectrum. In the FPO formalism, the closed system becomes open because of a really existing coupling between the localized closed system and the reservoir, i.e., because of the coupling between the Q and P subspaces. Due to this coupling, some discrete states of the closed system become resonance states of the open system which, in general, have finite life times.

In the present paper we are interested, above all, in the properties of the effective non-Hermitian Hamiltonian of the open quantum system, which acts on the Q subspace and carries the influence of the P subspace. It reads

$$H_{\text{eff}} = H_b + \sum_c V_{bc}\frac{1}{E^+ - H_c}V_{cb}. \quad (23)$$

Here, $E^+=E+i\epsilon$ with $\epsilon\to 0$. Further, V_{bc} and V_{cb} stand for the coupling operators between the Q subspace (described by H_b) and the P subspace (environment, described by H_c). The operator H_{eff} is non-Hermitian and describes the localized system under the influence of the reservoir [17].

The non-Hermitian operator H_{eff} is complex-symmetric and depends explicitly on energy. Its eigenvalues z_λ and eigenfunctions ϕ_λ,

$$(H_{\text{eff}} - z_\lambda)\phi_\lambda = 0, \quad (24)$$

are complex. The eigenvalues provide not only the energies of the resonance states but also their widths. The eigenfunctions are biorthogonal. For more details see [17].

We underline here that values like the S matrix and the cross section are independent of the manner how the Q and P subspaces are defined. However, in order to obtain the positions E_λ and widths Γ_λ of the resonance states from the eigenvalues z_λ of H_{eff}, the two subspaces have to be defined properly. Otherwise, the z_λ have nothing in common with the spectroscopic values $E_\lambda - i/2\Gamma_\lambda$ of the resonance states. This can be seen, e.g., from the fact that $\Gamma_\lambda\to 0$ if $Q+P\to Q$.

Using the FPO formalism, the scattering matrix S can be written in terms of the effective Hamiltonian and the external

scattering states $|E,c\rangle$ defined by $(H_c-E)|E,c\rangle=0$. It reads [4,17]

$$S_{cc'} = \delta_{cc'} - 2\pi i\langle E,c|V_{cb}\frac{1}{E-H_{\text{eff}}}V_{bc'}|E,c'\rangle. \quad (25)$$

Characteristic of Eq. (25) is that it contains H_{eff} with its explicit energy dependence. The energy dependence of H_{eff} plays an important role near decay thresholds and in the regime of overlapping resonances. The S matrix (25) is always unitary.

The FPO formalism may formally be considered as a certain generalization of the R matrix approach [45]. In both cases, the wave functions of the system are localized in coordinate space (Q subspace in the FPO formalism) and coupled to an extended continuum of scattering wave functions (P subspace in the FPO formalism). However, the standard spectroscopic parameters of the R matrix approach do not contain any feedback from the continuum of scattering wave functions. In the FPO formalism, they are replaced by the energy-dependent functions E_λ and Γ_λ in which the feedback from the continuum is involved.

We examine the concept of the effective Hamiltonian in connection with the potential scattering on spherically symmetric potentials. In order to define the Q subspace that contains the localized part of the problem, we truncate the potential at a certain cutoff radius R_{cut}. The P subspace is defined then by the remaining part of the function space being extended up to infinity. The operators V_{bc}, V_{cb} describe the coupling between the two subspaces. In this paper, we consider a one-dimensional (1D) quantum system to which one lead is attached at a certain point. We will describe such a system in the framework of the tight-binding approach.

B. One-dimensional tight-binding model for resonance scattering

Let us consider the resonance scattering on truncated Bargmann potentials V_{cut} as described in Secs. II and III following the FPO technique. We choose a radius R such that the functions defined at $0\leqslant r\leqslant R$ belong to the Q subspace, while the functions defined at $r>R$ belong to the P subspace. In order to describe the continuum (P subspace) properly, it should be $R\geqslant R_{cut}$.

A common approach to solve the Schrödinger equation in the context of the FPO formalism consists of the discretization of the spatial coordinate. The resulting matrix Hamiltonian is the so-called tight-binding Hamiltonian (see, e.g., [46]) which is widely used to model electronic transfer in molecules and condensed matter. To obtain the matrix representation for the effective Hamiltonian H_{eff} (23), we choose a discrete lattice whose points are located at $r=r_i=ia$, $i=1,\ldots,N$ ($r_N=R$) and approximate the second order derivative by the finite differences

$$\psi'' \approx \frac{1}{a^2}\{\psi_{i-1}-2\psi_i+\psi_{i+1}\}, \quad (26)$$

where $a=r_{i-1}-r_i$ is a lattice constant (being independent of i). Thus, for $r=r_i$, $i=1,\ldots,N-1$, we obtain the following finite-difference (or tight-binding) Schrödinger equation

$$t\{-\psi_{i-1}+2\psi_i-\psi_{i+1}\}+U_i\psi_i=E\psi_i, \quad (27)$$

where $U_i=V_{cut}(r_i)$ and $t=\frac{1}{a^2}$ is the tight-binding coupling constant.

Effects of scattering are introduced through the coupling between the box (Q subspace) and a semi-infinite lead (P subspace) that is attached at the point $R=r_N$. In order to describe these effects, we present the solution of the Schrödinger equation in the lead as

$$\psi_i = e^{-ikr_i} - S_{\text{FPO}}(k)e^{ikr_i}, \quad i\geqslant N. \quad (28)$$

This equation defines the one-channel scattering matrix $S_{\text{FPO}}(k)$. In the above equation we use the standard dispersion relation of the tight-binding model,

$$E = t[2-2\cos(ka)], \quad (29)$$

where a is the lattice constant (see above) and E is the real energy of the system. At $r=r_N$, where the Q subsystem (box) is coupled to the P subsystem (semi-infinite lead), the Schrödinger equation (27) takes the form [5,47]

$$t\{-\psi_{N-1}+(2-e^{ika})\psi_N\} = E\psi_N - 2ite^{-ikr_N}\sin(ka). \quad (30)$$

Denoting $\Psi=(\psi_1,\psi_2,\ldots,\psi_{N-1},\psi_N)^T$, we get the matrix equation

$$(E-H_{\text{eff}})\Psi = [E-(H_b-\tilde{W})]\Psi = b, \quad (31)$$

with coupling matrix $\tilde{W}_{ij}=\delta_{iN}\delta_{jN}te^{ika}$ and

$$H_{\text{eff}} = \begin{pmatrix} U_1+2t & -t & 0 & \ldots & 0 & 0 & 0 \\ -t & U_2+2t & -t & \ldots & 0 & 0 & 0 \\ 0 & -t & U_3+2t & \ldots & 0 & 0 & 0 \\ \vdots & \vdots & \vdots & \ddots & \vdots & \vdots & \vdots \\ 0 & 0 & 0 & \ldots & -t & U_{N-1}+2t & -t \\ 0 & 0 & 0 & \ldots & 0 & -t & -te^{ika}+2t \end{pmatrix}, \quad b = \begin{pmatrix} 0 \\ 0 \\ 0 \\ \vdots \\ 0 \\ 2ite^{-ikr_N}\sin(ka) \end{pmatrix}. \quad (32)$$

Equation (32) gives us the desired matrix representation for the effective non-Hermitian Hamiltonian H_{eff}. The Hamiltonian H_{eff} obtained from the above pictorial derivation is completely equivalent to the overall Green function derived in [46]. The matrix equation (31) describes the scattering on the discretized 1d quantum system with Bargmann potential at $r_i < R_{cut}$ and zero potential at $r_i \geqslant R_{cut}$ and with $R=R_{cut}=r_N$.

Although the poles of the S matrix are of no relevance for the scattering and reaction processes in the FPO formalism [16,17], it is interesting to estimate their value. This can be done by using the following standard method [3]. First, the fixed-point equations for the positions of the resonance states in energy are solved,

$$E_\lambda = \text{Re}[z_\lambda]|_{E=E_\lambda}, \tag{33}$$

and then the widths are defined by

$$\Gamma_\lambda = 2\,\text{Im}[z_\lambda]|_{E=E_\lambda}. \tag{34}$$

The solutions of these equations provide approximately the energies E_λ and widths Γ_λ of the resonance states as long as the Γ_λ are small. In the following, we call the solutions of Eqs. (33) and (34) shortened the *fixed-point solutions*.

In order to make a meaningful comparison of the results of the FPO method with those of the exactly solvable potentials, the poles of the S matrix obtained by using the FPO formalism should be determined exactly. This can be done by solving the equation

$$\text{Det}[E - H_{\text{eff}}(E)] = 0 \tag{35}$$

in the complex E plane, which follows from the expression (25), provided that V_{bc} and V_{cb} do not have poles. Equation (35) differs from an eigenvalue equation since the effective Hamiltonian depends on energy. We found the solutions of Eq. (35) by determining the intersection of contour lines for the zero values of the real and imaginary parts of the determinant. In order to distinguish the solutions of Eq. (35) from the fixed-point solutions, we call them *S matrix poles* in the following.

Using the S matrix obtained from Eqs. (31) and (28) we calculate the phase shift according to its definition (16),

$$\delta_{\text{FPO}}(k) = -\frac{i}{2}\ln S_{\text{FPO}}(k). \tag{36}$$

In all our numerical calculations presented in the next section, the lattice constant a is chosen to be 0.01. We performed calculations also with $a=0.001$. These calculations require much more computer resources and change the results only slightly. The fixed-point equations are solved for $R=R_{cut}$.

V. RESULTS

A. One-resonance potential

To illustrate the differences between physical (resonance) poles and unphysical (cutoff) poles more specifically we first apply the method described in Sec. II to construct a potential with one resonance state. This allows us to carry out a simultaneous comparative analysis of the smooth (nontruncated) potential, its truncated version (both obtained with the help of SUSY technique) and their cutoff counterpart resulting from the FPO formalism.

Our choice $V_0(r)=0$ in Eq. (9), which allows us to use solutions of the free particle Schrödinger equation, simplifies the calculations considerably. A resonance is obtained when two irregular transformation functions of type (11) with real parameters a_1 and a_2 are used in a chain of transformations, i.e.,

$$u_1 = \exp(-i\alpha_1 r) \equiv \exp[(a_1 + ia_2)r],$$

$$u_2 = \exp(-i\alpha_2 r) \equiv \exp[(a_1 - ia_2)r]. \tag{37}$$

As regular solutions (11) we choose, in the current case, hyperbolic sine functions

$$v_1 = \sinh(b_1 r), \quad v_2 = \sinh(b_2 r). \tag{38}$$

The real constants a_i, b_i should be such that $b_i > 0$, $a_2 < a_1 < 0$. The desired potential follows from Eq. (9) where we have to calculate a fourth order Wronskian $W(u_1,u_2,v_1,v_2)$. The calculations are simplified if we notice that this fourth order Darboux transformation is equivalent to a set of two first order transformations and one second order transformation. If we choose for the first transformation the transformation function $u=u_1$, it results, according to Eqs. (4) and (5), in the zero potential difference (i.e., the initial potential remains the potential of the free particle). Then we have to change only the form of the three other transformation functions. These functions become L_1u_2, L_1v_1, L_1v_2 with $L=L_1$ given by Eq. (2) where $w=-i\alpha_1$. Evidently, the function L_1u_2 is, up to an inessential constant factor, the same exponential as u_2, and the functions L_1v_1, L_1v_2 become proportional to hyperbolic cosines with shifted arguments. For the second transformation we choose the transformation function L_1u_2 which still does not add anything to the zero potential but changes the transformation functions $L_1v_1 \to L_2L_1v_1$ and $L_1v_2 \to L_2L_1v_2$ [here L_2 is given by the same formula (2) with $w=-i\alpha_2$], producing additional shifts in their arguments. After that we realize the second order transformation with the transformation functions

$$L_2L_1v_1 \sim \sinh(b_1 r - \zeta_1), \quad L_2L_1v_2 \sim \sinh(b_2 r - \zeta_2), \tag{39}$$

where

$$\tanh\zeta_i = \frac{2a_1b_i}{b_i^2 + a_1^2 + a_2^2}, \quad i = 1,2 \tag{40}$$

which gives the desired one-resonance potential

$$V_{1res} = \frac{2(b_1^2 - b_2^2)[b_2^2 \sinh(b_1 r - \zeta_1)^2 - b_1^2 \sinh(b_2 r - \zeta_2)^2]}{[b_2 \sinh(b_1 r - \zeta_1)\cosh(b_2 r - \zeta_2) - b_1 \sinh(b_2 r - \zeta_2)\cosh(b_1 r - \zeta_1)]^2}. \quad (41)$$

The potential V_{1res} (see Fig. 1, dashed line) represents a generalization of a two-soliton potential defined on the positive semiaxis [48]. Instead of two discrete levels, present in the two-soliton potential, the potential (41) has one resonance state.

The Jost function (13) reads

$$F_{1res} = \frac{(k - \alpha_1)(k - \alpha_2)}{(k + ib_1)(k + ib_2)}. \quad (42)$$

Hence the resonance occurs at $k = \alpha_1 = -a_2 + ia_1$ with the mirror pole at $k = \alpha_2 = a_2 + ia_1$, $a_i < 0$, $i = 1, 2$.

The phase shift (17) is now given by

$$\delta_{1res} = -\arctan \frac{2a_1 k}{a_1^2 + a_2^2 - k^2} - \arctan \frac{k(b_1 + b_2)}{b_1 b_2 - k^2}. \quad (43)$$

To be able to compare the results obtained by the two different methods, we draw all figures in the E plane [$E = k^2$ for continuum and Eq. (29) in the tight-binding case].

First we compare the scattering phase shift (36) calculated by means of FPO technique with that calculated by Eq. (43); Fig. 2. The agreement of Eq. (36) with the exact result (43) holds true up to high energy values and in a large range of cutoff radii. Even in the middle of tight-binding conductance band $E = 2/t$, where we cannot expect good agreement between continuous and tight-binding models, the difference $\delta_{1res} - \delta_{\mathrm{FPO}}$ does not exceed 0.1. The inset of Fig. 2 shows the difference between the values of the exact phase shift δ and the numerical δ_{FPO}. The maximum difference occurs near the resonance position.

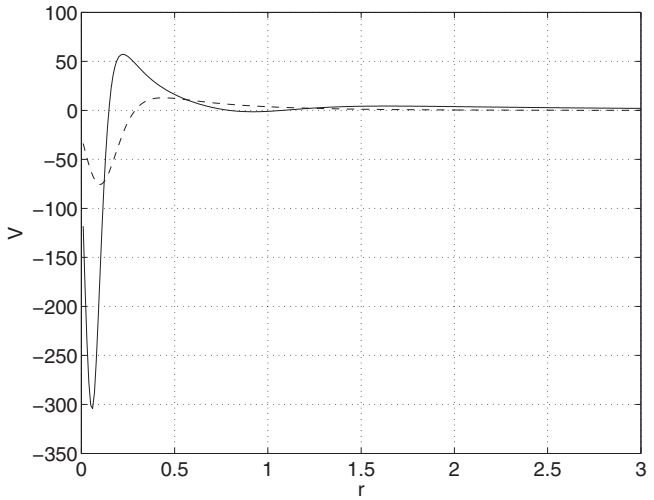

FIG. 1. One-resonance Bargmann-type potential (dashed line) at $a_1 = -0.1$, $a_2 = -2$, $b_1 = 1$, and $b_2 = 2$. Two-resonances potential (solid line) at $a_1 = -0.1$, $a_2 = -2$, $a_3 = -0.08$, $a_4 = -3$, $b_1 = 0.2$, $b_2 = 0.1$, $b_3 = 0.08$, and $b_4 = 0.05$.

According to Eq. (43), the phase shift is a sum of two terms. When the parameter values are those used in Fig. 2, both terms contribute with comparable weight even in the very neighborhood of the resonance. For other parameter values (e.g., $a_1 = -0.01$, $a_2 = -2$ for the resonance term and $b_1 = 100$, $b_2 = 200$ for the background), one term dominates in the neighborhood of the resonance and the phase shift is the standard one (i.e., π) in this energy region.

Let us now analyze the calculated spectroscopic data. As shown in [49], a cutoff potential produces a chain of poles of the S matrix and there are no poles lying below this chain in the complex plane. A narrow physical resonance of the nontruncated potential separates from the chain of cutoff poles. It is chosen to lie close to the real energy axis.

Figure. 3 shows all poles ($\mathrm{Re}[E] < 100$) generated by the potential (41) truncated at $R_{cut} = 5$. The roots of transcendental equation (22) are shown as circles, the crosses present the distribution of complex solutions of Eq. (35), and daggers stand for the results of the fixed-point approximation (33) and (34). The resonance which is due to the nontruncated potential (41) is clearly separated from the cutoff poles. Its exact value is $E = (-a_2 + ia_1)^2 = 3.99 - i0.4$. The fixed-point approximation (34) gives the width of the poles with a significant error. The S matrix pole (35) reproduces this value to a high precision (relative error is less than 1% for shown poles).

The picture related to the cutoff poles is, according to Fig. 3, the following: the S matrix poles (35) coincide with the roots of transcendental equation (22), whereas the widths (34) obtained by using the fixed-point approximation are far too small. That means that all poles of the S matrix are very good reproduced by the solutions of Eq. (35). The fixed-

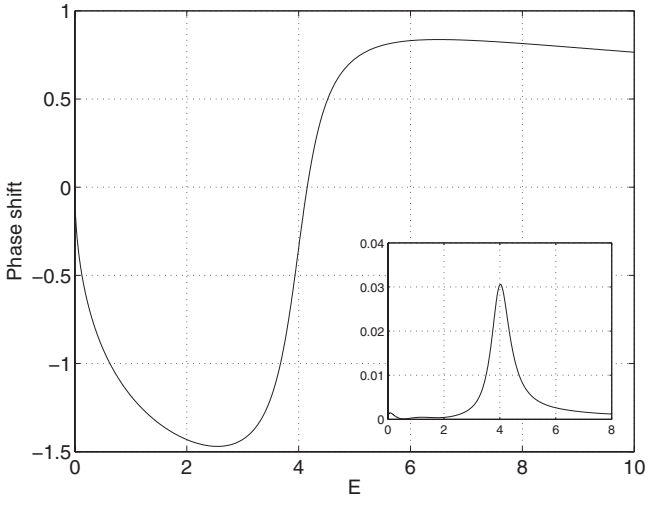

FIG. 2. Phase shift for one-resonance potential at $a_1 = -0.1$, $a_2 = -2$, $b_1 = 1$, $b_2 = 2$, and $R_{cut} = 5$. Inset shows the difference between δ_{1res} and δ_{FPO}.

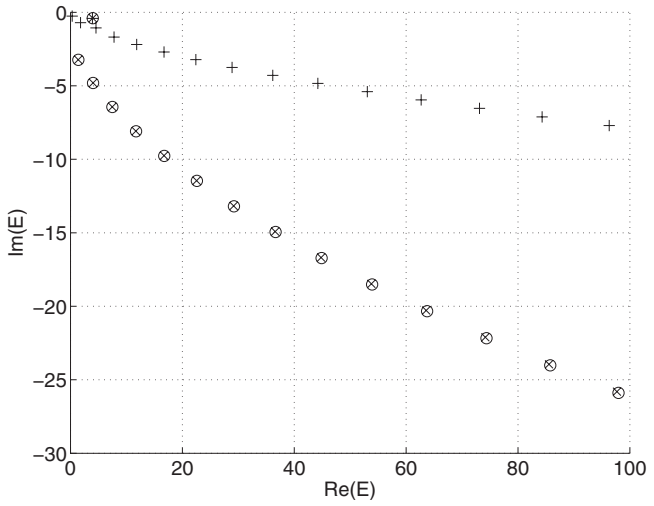

FIG. 3. Poles of the truncated one-resonance potential at $a_1=-0.1$, $a_2=-2$, $b_1=1$, $b_2=2$ and cutoff radius $R_{cut}=5$. The symbols correspond to the roots of transcendental equation (22) (○), the poles of the S matrix obtained from Eq. (35) (×), and the fixed-point approximation (33) and (34) (+).

point approximation (33) allows one to accurately determine only the position of narrow resonances. This result agrees with the definitions (33) and (34) according to which the fixed-point equation is solved only for the real energy.

In order to see how the resonance of the nontruncated potential separates from the chain of cutoff poles one can consider the dependence of the pole location on the cutoff radius R_{cut}. Indeed, only the physical resonance is almost independent of R_{cut}. All the other poles move if the cutoff radius is changed.

To show this dependence in detail we present the results from a set of calculations by using the FPO technique for different cutoff radii R_{cut}. First we consider the fixed-point approximation (Figs. 4 and 5). The trajectory of one of the eigenvalues has a strongly pronounced bight. The eigenvalue trajectory is spiraling around the correct value of the physical resonance ($E=3.99-i0.4$), see Fig. 4. For the broader resonance ($E=3.96-i0.8$) shown in Fig. 5 the spiraling trajectory has less rotations and the localization of the resonance value becomes more difficult. As a result, the fixed-point approximation correctly indicates the position of the narrow resonance only.

Figure 6 shows the solutions of Eq. (35). They show a similar dependence on R_{cut} as the fixed-point solutions (Figs. 4 and 5). However, the S matrix poles obtained by solving both Eqs. (35) and (22) coincide. The trajectory of one of the poles converges very quickly to the resonance value along the spiraling trajectory.

The results shown in Figs. 4–6 demonstrate that the cutoff trajectories of the fixed-point solutions (33) and (34) and of the S matrix poles (35) depend strongly on R_{cut}. The spiraling trajectories of the physical resonances arise from a lot of avoided crossings of the trajectories of neighboring cutoff trajectories. On this account, the spectroscopic values of the physical resonances are influenced only a little by varying R_{cut}. The resonance location in Fig. 6 is stable with $R_{cut}\rightarrow 7$ in contrast to those in Figs. 4 and 5.

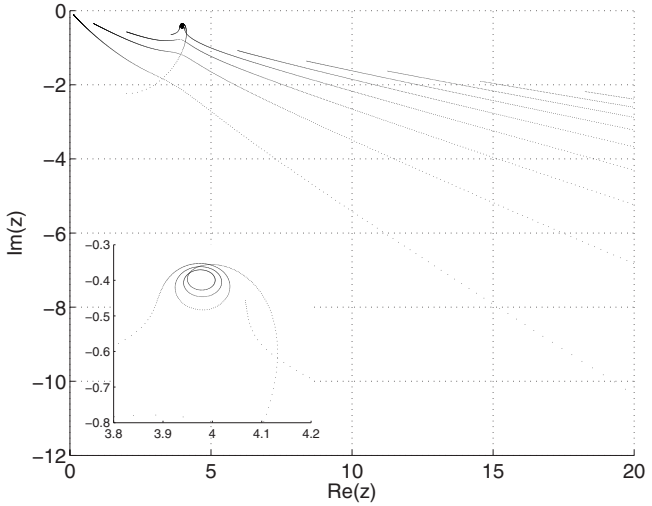

FIG. 4. Solutions of fixed-point equations (33) and (34) for one-resonance potential at $a_1=-0.1$, $a_2=-2$, $b_1=1$, and $b_2=2$. Cutoff radius R_{cut} changes from 0.5 to 7 with step 0.01. With increasing R_{cut}, the trajectories move to small $\mathrm{Re}(z)$, $|\mathrm{Im}(z)|$ (with the exception of the spiraling trajectory).

B. Two-resonance potential

Let us now consider the more complicated case of a potential supporting two resonance states. To construct the Bargmann-type potential (see Sec. II) we are using eight transformation functions. As four irregular solutions from the set (11) we choose two functions (37) with $a_2<a_1<0$ and the following two functions:

$$u_3=\exp(-i\alpha_3 r)\equiv\exp[(a_3+ia_4)r],$$

$$u_4=\exp(-i\alpha_4 r)\equiv\exp[(a_3-ia_4)r] \tag{44}$$

with $a_3<a_4<0$. As four regular solutions we choose two functions (38) and

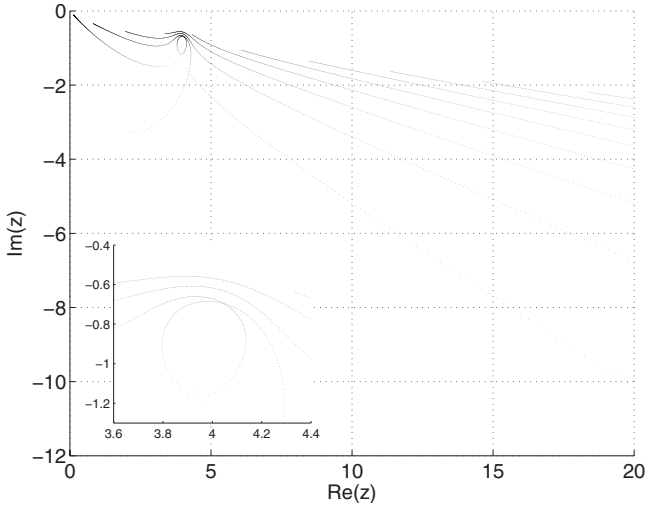

FIG. 5. Solutions of fixed-point equations (33) and (34) for one-resonance potential at $a_1=-0.2$, $a_2=-2$, $b_1=1$, and $b_2=2$. Cutoff radius R_{cut} changes from 0.5 to 7 with step 0.01. With increasing R_{cut}, the trajectories move to small $\mathrm{Re}(z)$, $|\mathrm{Im}(z)|$ (with the exception of the spiraling trajectory).

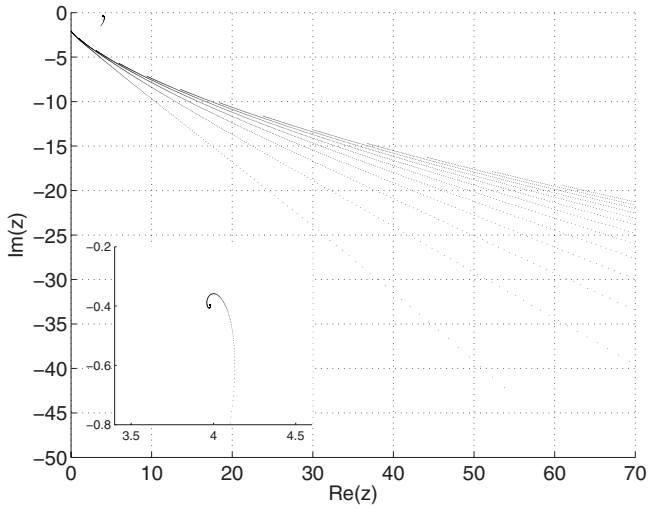

FIG. 6. Trajectories of S-matrix poles (35) for one-resonance potential at $a_1=-0.1$, $a_2=-2$, $b_1=1$, and $b_2=2$. Cutoff radius R_{cut} changes from 0.5 to 7 with step 0.01. With increasing R_{cut}, the trajectories move to small $\mathrm{Re}(z)$, $|\mathrm{Im}(z)|$ (with the exception of the spiraling trajectory).

$$v_3 = \sinh(b_3 r), \quad v_4 = \sinh(b_4 r) \tag{45}$$

with all $b_i > 0$. The desired potential follows from Eq. (9) where this time an eighth order Wronskian should be calculated. To simplify calculations we replace, similar to the previous section, the eighth order Darboux transformation by a chain of four first order transformations, involving exponential transformation functions only, and one fourth order transformation. The first order transformations keep unchanged the zero initial potential but affect the hyperbolic transformation functions, producing only shifts in their arguments. Thus the potential is calculated by Eq. (9) with $V_0=0$ and the fourth order Wronskian $W(\tilde{v}_1,\ldots,\tilde{v}_4)$. Here $\tilde{v}_i=\sinh(b_i r - \eta_i)$, $\eta_i=\zeta_i+\tilde{\zeta}_i$ where ζ_i for $i=3,4$ are calculated by Eq. (40) and $\tilde{\zeta}_i$ for $i=1,\ldots,4$ are calculated by the same formula with a_1 and a_2 replaced by a_3 and a_4. After some calculations we obtain an explicit expression for the Wronskian,

$$W(\tilde{v}_1,\ldots,\tilde{v}_4) = \sum_{i=1}^{3}\sum_{j=i+1}^{4} (-1)^{i+j} b_i b_j (b_j^2 - b_i^2) \times (b_k^2 - b_l^2)\cosh\xi_i \cosh\xi_j \sinh\xi_k \sinh\xi_l, \tag{46}$$

where $\xi_i=b_i r-\eta_i$ and, in every term, $k>l$ take the values from the set (1,2,3,4) different from the values of i and j. An explicit expression for the obtained potential is rather involved and we omit it here. Its typical behavior is shown on Fig. 1, solid line.

The Jost function for the two resonance potential follows from Eq. (13),

$$F_{2res} = \prod_{j=1}^{4} \frac{k-\alpha_j}{k+ib_j}. \tag{47}$$

Thus the resonances occur at $k=k_1=-a_2+ia_1$ and $k=k_2=-a_3+ia_4$ with the mirror poles at $k=a_2+ia_1$ and $k=a_3+ia_4$.

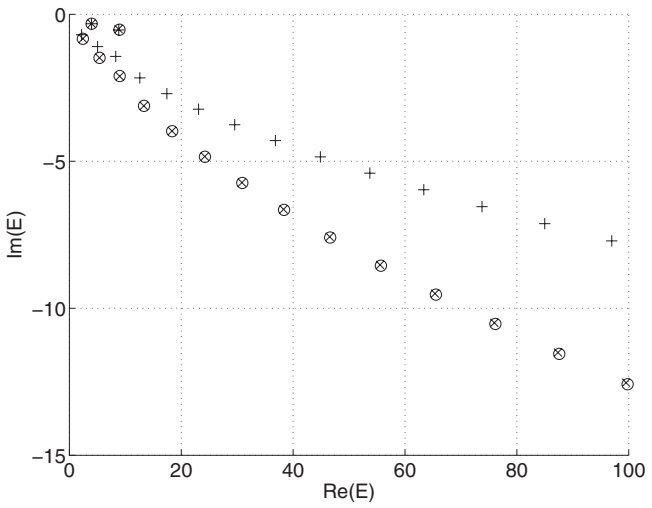

FIG. 7. Poles of the truncated two-resonance potential at $a_1=-0.1$, $a_2=-2$, $a_3=-0.08$, $a_4=-3$, $b_1=0.2$, $b_2=0.1$, $b_3=0.08$, $b_4=0.05$, and cutoff radius $R_{cut}=5$. The symbols correspond to the roots of transcendental equation (22) (○), the poles of the S matrix (35) obtained from the eigenvalues of H_{eff} (×), and the fixed-point approximation (33) and (34) (+).

The resonance behavior of the cross section is more visible when S-matrix poles are close enough to the real axis. This is achieved by a proper choice of the Bargmann potential parameters. Results of our calculations are presented in Figs. 7–9. For the set of parameters chosen in these figures the complex energies have the values

$$E_1 = (-a_2 + ia_1)^2 = 3.99 - i0.4$$

and

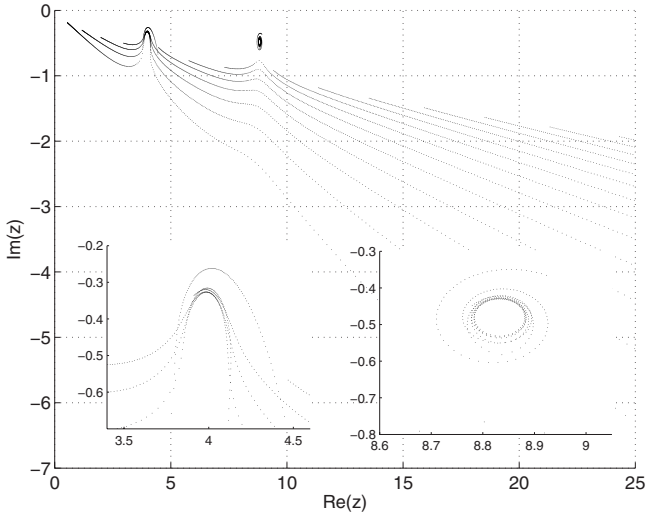

FIG. 8. Solutions of fixed-point equations (33) and (34) for two-resonance potential $a_1=-0.1$, $a_2=-2$, $a_3=-0.08$, $a_4=-3$, $b_1=0.2$, $b_2=0.1$, $b_3=0.08$, $b_4=0.05$. Cutoff radius R_{cut} changes from 0.5 to 7 with step 0.01. With increasing R_{cut}, the trajectories move to small $\mathrm{Re}(z)$, $|\mathrm{Im}(z)|$ (with the exception of the spiraling trajectory).

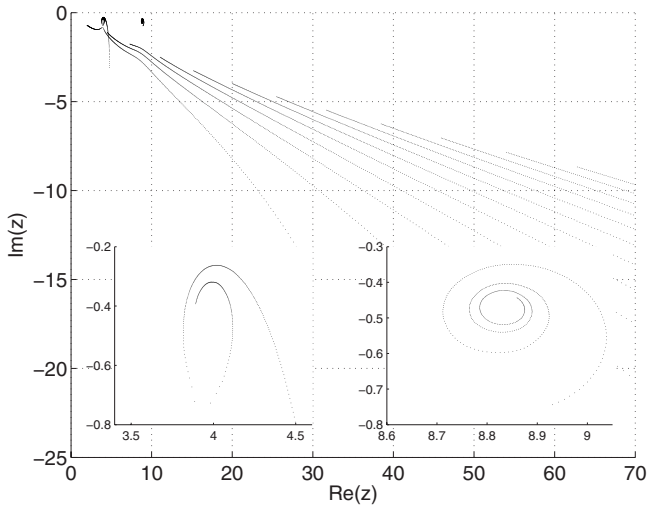

FIG. 9. Trajectories of S-matrix poles (35) for two-resonance potential at $a_1=-0.1$, $a_2=-2$, $a_3=-0.08$, $a_4=-3$, $b_1=0.2$, $b_2=0.14$, $b_3=0.08$, and $b_4=0.05$. Cutoff radius R_{cut} changes from 0.5 to 7 with step 0.01. With increasing R_{cut}, the trajectories move to small $\mathrm{Re}(z)$, $|\mathrm{Im}(z)|$ (with the exception of the spiraling trajectory).

$$E_2 = (-a_4 + ia_3)^2 = 8.9936 - i0.48.$$

The figures show the same features as those obtained for the one-resonance case. Two narrow resonances stand separately from the chain of the cutoff poles. The poles of the S matrix are determined well enough when calculated according to Eq. (35). Solutions of the fixed-point approximation (33) identify correctly the positions of the physical poles if they are close enough to the real axis.

VI. CONCLUSION

In the present paper, we considered the application of the FPO formalism to potential scattering in the single-channel case. For this purpose we analytically constructed model potentials being a generalization of Bargmann potentials to resonance states with one and two resonances at given energies.

In the FPO formalism, the corresponding spectroscopic and scattering information is obtained from the non-Hermitian Hamiltonian H_{eff} and the S matrix derived by means of H_{eff}. The Hamiltonian H_{eff} describes the localized part of the system under the influence of the coupling to the continuum. In the present paper, it is obtained in the framework of the tight-binding model.

First we compared the phase shifts obtained numerically in both methods. We received an astonishing good agreement of the results obtained in the two models. The phase shift notifies only the physical resonances.

To compare the spectroscopic values obtained in the two models, we are confronted with the problem that the eigenvalues of H_{eff} involved in the S matrix are energy dependent while the exactly solvable potentials provide us only the poles of the S matrix. We therefore have to determine the poles of the S matrix also in the framework of the FPO formalism. The standard fixed-point approximation (33) for the positions of the resonances is inadequate for this purpose since the widths are determined by solving Eq. (34) at the positions of the resonances. Hence the widths are, generally, erroneous. The results of our calculations show clearly that the fixed-point approximation gives, nevertheless, reasonable values if the widths are small enough. In order to determine exactly the poles of the S matrix in the framework of the FPO formalism, we solved the nonlinear equation (35), $\mathrm{Det}[E-H_{\mathrm{eff}}(E)]=0$, in the complex E plane.

The results for the spectroscopic values are the following. The truncation of the potential in the tight-binding FPO model leads to the appearance of spurious solutions of Eq. (35) just as in the well-known case of the S-matrix cutoff poles [22]. The physical resonances of the truncated Bargmann potentials are well described by the complex energies satisfying Eq. (35), i.e., by the S matrix poles calculated in the FPO formalism. Furthermore, the spurious solutions coincide with the cutoff poles of the scattering matrix. The last ones behave differently from the physical resonances in repeated calculations with different parameter sets. In our case the parameter is the cutoff radius R_{cut} (the potential is set to zero at coordinates $r \geqslant R_{cut}$). The physical poles representing visual resonances are stable against variation of R_{cut}, in a certain range, in contrast to the cutoff poles that are not stable.

ACKNOWLEDGMENTS

V.V.S. acknowledges support from INTAS Grant No. 06-1000016-6264. V.V.S. and B.F.S. are partially supported by Grants Nos. RFBR-06-02-16719 and SS-871.2008.2. V.V.S. and K.N.P. are grateful to the MPIPKS Dresden for hospitality.

[1] H. Feshbach, Ann. Phys. (N.Y.) **5**, 357 (1958).
[2] H. Feshbach, Ann. Phys. (N.Y.) **19**, 287 (1962).
[3] H. W. Barz, I. Rotter, and J. Höhn, Nucl. Phys. A **275**, 111 (1977).
[4] I. Rotter, Ann. Phys. (Leipzig) **493**, 221 (1981).
[5] A. F. Sadreev and I. Rotter, J. Phys. A **36**, 11413 (2003).
[6] I. Rotter and A. F. Sadreev, Phys. Rev. E **69**, 066201 (2004).
[7] I. Rotter and A. F. Sadreev, Phys. Rev. E **71**, 036227 (2005).
[8] I. Rotter and A. F. Sadreev, Phys. Rev. E **71**, 046204 (2005).
[9] A. F. Sadreev, E. N. Bulgakov, and I. Rotter, Phys. Rev. B **73**, 235342 (2006).
[10] E. N. Bulgakov, I. Rotter, and A. F. Sadreev, Phys. Rev. E **74**, 056204 (2006).
[11] E. N. Bulgakov, I. Rotter, and A. F. Sadreev, Phys. Rev. B **76**, 214302 (2007).
[12] A. I. Magunov, I. Rotter, and S. I. Strakhova, J. Phys. B **32**, 1489 (1999).
[13] A. I. Magunov, I. Rotter, and S. I. Strakhova, J. Phys. B **32**,

1669 (1999).
[14] A. I. Magunov, I. Rotter, and S. I. Strakhova, J. Phys. B **34**, 29 (2001).
[15] Y. V. Fyodorov and H.-J. Sommers, J. Math. Phys. **38**, 1918 (1997).
[16] I. Rotter, Rep. Prog. Phys. **54**, 635 (1991).
[17] J. Okołowicz, M. Płoszajczak, and I. Rotter, Phys. Rep. **374**, 271 (2003).
[18] J. Humblet, Mem. Soc. R. Sci. Liege Collect. in-8 **12**, 4 (1952).
[19] T. Regge, Nuovo Cimento **8**, 671 (1958).
[20] R. G. Newton, *Scattering Theory of Waves and Particles* (Springer-Verlag, New York, 1982).
[21] L. D. Faddeev, Usp. Mat. Nauk **14**, 57 (1959); J. Math. Phys. **4**, 72 (1963).
[22] H.-D. Meyer and O. Walter, J. Phys. B **15**, 3647 (1982).
[23] W. Domcke, Phys. Rev. A **28**, 2777 (1983).
[24] W. Domcke, M. Berman, C. Mundel, and H.-D. Meyer, Phys. Rev. A **33**, 222 (1986).
[25] D. V. Savin, V. V. Sokolov, and H.-J. Sommers, Phys. Rev. E **67**, 026215 (2003).
[26] V. I. Kukulin, V. M. Krasnopolsky, and J. Horáček, *Theory of Resonances. Principles and Applications* (Kluwer, Dordrecht, 1989).
[27] E. Witten, Nucl. Phys. B **188**, 513 (1981).
[28] K. Chadan and P. C. Sabatier, *Inverse Problems in Quantum Scattering Theory* (Springer, Berlin, 1977).
[29] V. G. Bagrov and B. F. Samsonov, Theor. Math. Phys. **104**, 356 (1995).
[30] V. Bargmann, Rev. Mod. Phys. **21**, 488 (1949).
[31] B. F. Samsonov, J. Phys. A **28**, 6989 (1995).
[32] A. A. Andrianov and A. V. Sokolov, J. Math. Sci. (N.Y.) **143**, 2707 (2007) [Zap. Nauchn. Semin. POMI **335**, 22 (2006)].
[33] A. V. Sokolov, Zap. Nauchn. Semin. POMI **347**, 214 (2007).
[34] A. A. Andrianov, M. V. Ioffe, and D. N. Nishnianidze, Phys. Lett. A **201**, 103 (1995).
[35] A. A. Andrianov, M. V. Ioffe, and V. Spiridonov, Phys. Lett. A **174**, 273 (1993).
[36] V. G. Bagrov and B. F. Samsonov, Phys. Part. Nucl. **28**, 374 (1997).
[37] G. Junker, *Supersymmetric Methods in Quantum and Statistical Physics* (Springer, Berlin, 1996).
[38] F. Cooper, A. Khare, and U. Sukhatme, *Supersymmetry in Quantum Mechanics* (World Scientific, Singapore, 2001).
[39] B. K. Bagchi, *Supersymmetry in Quantum and Classical Mechanics* (Chapman and Hall, New York, 2001).
[40] B. Mielnik and O. Rosas-Ortiz, J. Phys. A **37**, 10007 (2004).
[41] B. F. Samsonov and F. Stancu, Phys. Rev. C **66**, 034001 (2002).
[42] M. N. Crum,Q. J. Math. **6**, 121 (1955).
[43] P. Roman, *Advanced Quantum Theory* (Addison-Wesley, Reading, MA, 1965).
[44] L. E. Ballentine, *Quantum Mechanics: A Modern Development* (World Scientific Publishing Company, Singapore, 1998).
[45] I. Rotter, Acta Phys. Pol. B **35**, 1269 (2004).
[46] S. Datta, *Electronic Transport in Mesoscopic Systems* (Cambridge University Press, Cambridge, England, 1995).
[47] T. Ando, Phys. Rev. B **44**, 8017 (1991).
[48] V. B. Matveev and M. A. Salle, *Darboux Transformations and Solitons* (Springer, Berlin, 1991).
[49] H. M. Nussenzweig, Nucl. Phys. **11**, 499 (1959); H. M. Nussenzweig, *Causality and Dispersion Relations* (Academic, New York, 1972).